# Assessing ionospheric convection estimates from coherent scatter from the radio aurora

Enrique Rojas  David Hysell

Cornell University

## Abstract

The Doppler spectra obtained from coherent radar backscatter from auroral E region plasma irregularities, combined with an empirical model, provide a way to estimate auroral convection patterns. These estimates are consistent with rocket, optical and incoherent scatter radar data, but direct comparison between the different datasets are not straightforward. In this work, we evaluate the physical consistency of the estimated fields: the model will be satisfactory to the extent that the convection patterns derived from them are incompressible. The results suggest that the evaluated convection patterns are consistently incompressible within experimental uncertainties.

## I. Introduction

Radar aurora can be studied with high precision and spatiotemporal resolution using small coherent radars. This systems can measure echoes from irregularities in the plasma, which are related with other physical parameters of the plasma, through known empirical models [1].

We propose a way to assess the mathematical and physical consistency of the model. Since the convection electric field is electrostatic, the convection pattern must be close to incompressible. Given that the empirical model does not contain any explicit assumption of incompressibility, we argue that if the convection field satisfies $\nabla \cdot v_d \approx 0$ within experimental error, then the model estimates are accurate.

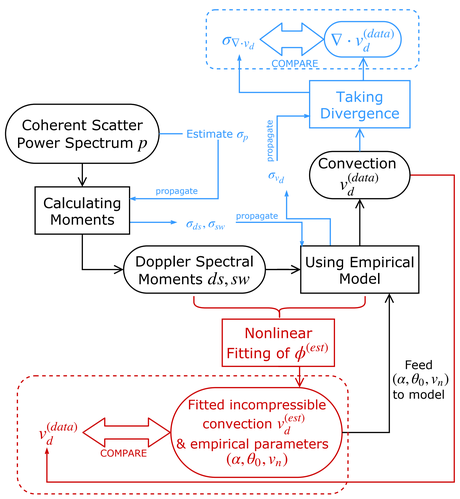


Figure 1 – Data Processing Flow. Black: Calculation of convection field from spectral moments. Blue: Error propagation to assess whether the fields are incompressible within experimental uncertainty. Red: Fitting of incompressible convection fields to spectral moments data.

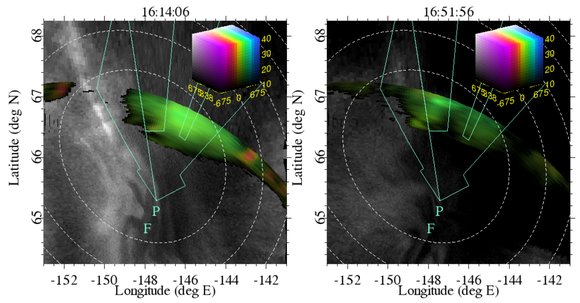


Figure 2 – Representative radar and all–sky imagery for different times during the Dec. 20, 2015 substorm. Radar data are represented by colored pixels: brightness, hue and saturation indicates SNR, Doppler shift and spectral width respectively.

## II. Empirical Model and Inversion Method

We can infer the auroral convection field wherever coherent scatter data are available using the empirical relations [1]:

$$ds = \left[350 + \left(\frac{v_d}{100}\right)^2\right] \cos(\theta - \theta_0) + v_n \quad (1)$$

$$sw = \alpha \left[350 + \left(\frac{v_d}{100}\right)^2\right] |\sin(\theta - \theta_0)| \quad (2)$$

where $ds$ is the Doppler shift, $sw$ the spectral width, $v_d$ the convection speed, $\theta$ the flow angle, $\theta_0$ a correction term to account for wave turning effects, and $v_n$ models the influence of neutral winds.

If $\vec{E}^{(data)}$ and $\vec{E}^{(\text{est})}$ are the electric fields obtained from the spectral data and fitting estimates respectively, the potential that satisfies

$$\phi^{(est)} = \min_{\phi} \|\vec{E}^{(\text{data})} - \vec{E}^{(\text{est})}(ds, sw)\|^2 + \beta \|\nabla\phi\|^2 \quad (3)$$

will minimize its discrepancy with the data and its curvature at the same time. $\beta$ is a regularization parameter. Eqn (3) was solved using the Levenberg–Marquardt method.

## III. Estimation of Flows

Optimal $(\alpha, v_n, \theta_0)$ were obtained from the L-curve analysis (Figure 3). Figure 4 shows a superposition of the Doppler spectral moments, the convection fields calculated from the Doppler spectra measurements, and the inverted potential pattern. The produced fields follow the fitted equipotential lines as expected. Moreover, the magnitudes of the convection and potential patterns are consistent with previous experiments

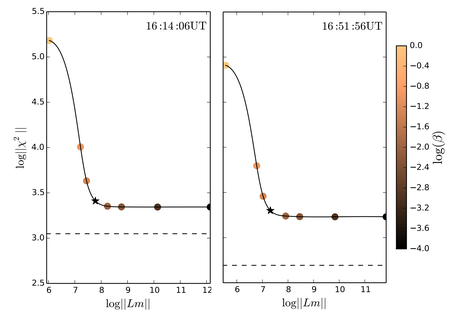


Figure 3 – L-curves for different times. The circles indicate the points obtained from the inversion process. The dashed line indicates the expected $\|\chi\|^2$ from the discrepancy principle and the star indicates the point of maximum curvature.

## IV. Assessing Incompressibility

Figure 3 shows L-curves for the times depicted on the Doppler image. All the optimal regularization parameters for these and the rest of the L-curves for the December 20, 2015 substorm [1] were between 0.01 and 0.03. At the point of maximum curvature, $\|\chi\|^2$ is consistently on the same order of magnitude of the value expected from the discrepancy principle. The distributions of $|\nabla \cdot v_d|$ are shown in Figure 5. A representative value of the expected uncertainty of the divergence due to error propagation ($\sigma_{\nabla\cdot v_d}$) was obtained from Eqns. (1) and (2) [1]. $A_{\text{Out}}$ and $A_{\text{Total}}$ correspond to the area under the curve to the left of $\sigma_{\nabla\cdot v_d}$ and to the total area respectively. Consequently, $A_{\text{Out}}/A_{\text{Total}}$ estimates the number of instances where the empirical model failed to produce incompressible regions.

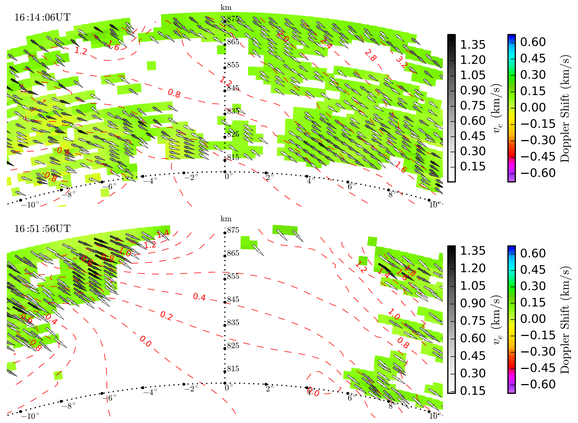


Figure 4 – Convection Patterns. The background colored bins corresponds to $ds$, the dashed red lines to the equipotential lines (kV) and the vector field to $v_d$. The radial axis accounts for the range and the azimuthal axis for the angular span of the field of view of the radar.

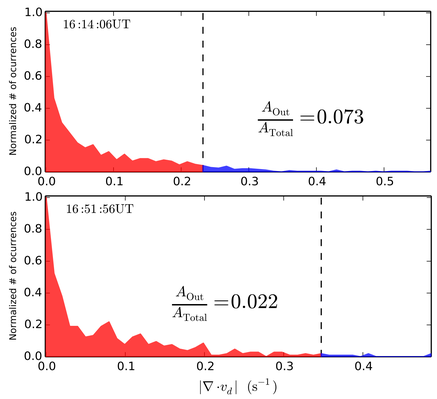


Figure 5 – Distribution of divergence magnitudes for different times. The horizontal axis represents the range of magnitudes of $|\nabla \cdot v_d|$ at each indicated time. The dashed lines indicate the positions of the estimated error propagated into the calculation of the divergence ($\sigma_{\nabla\cdot v_d}$). The red and blue areas correspond to the fraction of divergence magnitudes below and above $\sigma_{\nabla\cdot v_d}$, respectively.

## V. Discussion and Future Work

Figure 5 suggest that Eqns. (1) and (2) produce essentially incompressible flow fields. Furthermore, the estimated $\sigma_{\nabla\cdot v}$ represents a lower bound for the estimated uncertainty of the divergence, which means that the actual uncertainty may be larger [1]. Further research will relax the assumption that $v_n$ is constant which may account for the difference between the point of maximum curvature of the L-curves and the values expected from the discrepancy principle. Likewise, future work will address the conditions that have to be satisfied to trust the convection patterns obtained from the potential patterns in regions with little or no data.

## Conclusions

- Comparisons between convection patterns derived from spectral moments and other data sets are difficult. New validation criteria are needed.
- We use the incompressible nature of the convection electric field to assess the consistency of the convection estimates.
- Error propagation and inversion analysis suggested that most of the convection fields are incompressible within experimental uncertainty.

## References

[1] Rojas, E., D. L., Hysell, Assessing ionospheric convection estimates from coherent scatter from the radio aurora, *(Submitted)*.